Rev. Roum. Sci. Techn.– Électrotechn. et Énerg.
Vol. **69**, *2*, pp. 135–140, Bucarest, 2024

VOLTAGE SENSORLESS CONTROL OF FIVE-LEVEL PACKED U-CELL INVERTER BASED ON LYAPUNOV APPROACH FOR GRID-CONNECTED PHOTOVOLTAIC SYSTEM

BOUTHEYNA HADMER[1], SAID DRID[2], ABDALLAH KOUZOU[3], LARBI CHRIFI-ALAOUI[4]

Keywords: Packed U-cell; Multilevel converter; Lyapunov control theory; Maximum power point tracking (MPPT).

This paper deals with the nonlinear control of a five-level packed U-Cell (PUC5) inverter used in a grid-on photovoltaic (PV) system. The sensorless modulation strategy is adopted to control the switching of the six power switches. This topology generates a five-level output voltage with fewer active and passive components than traditional multilevel inverters. A nonlinear controller was designed to control the grid current using the Lyapunov theorem to ensure the asymptotic stability of the overall system. The proposed control scheme addresses two key challenges: minimizing the injected grid current's total harmonic distortion (THD) while balancing the capacitor voltage at their reference under various operating conditions. The efficiency of the proposed approach was comprehensively evaluated using theoretical analysis, mathematical modeling, and simulation results obtained using MATLAB/Simulink software.

1. INTRODUCTION

In recent years, renewable energy sources have received great interest as a promising alternative to traditional ones. This interest has been fueled by the escalating levels of pollution and the depletion of non-renewable resources such as fossil fuels. Among the various forms of renewable energy, photovoltaic (PV) energy has gained significant traction and attention [1,2]. A multilevel inverter is required to connect and use the power generated by the solar panels [3]. This equipment component is crucial for converting the unregulated dc power produced by the solar panels into regulated ac power that households and industries can use. The multilevel inverter technology has evolved in recent years and has become an integral part of the renewable energy sector. It provides several key advantages, such as improved efficiency, better power quality, and the ability to operate in isolated and grid-connected systems. Therefore, developing and implementing multilevel inverters have become a key area of research in the renewable energy sector [4]. Several studies have been conducted to present various configurations of multilevel converters, such as flying capacitor (FC), cascaded H-bridge (CHB), and neutral point clamped (NPC) [5]. However, the main challenge with these topologies is that they require large power electronics and dc sources, leading to larger package sizes and higher manufacturing costs [6,7]. In addition, employing less isolated dc sources in the rapidly expanding PV power energy applications means fewer tracking algorithms, resulting in a simpler system structure [8,9].

The packed U-cell converter (PUC) is a promising topology for achieving high voltage levels with few capacitors, power switches, and separate DC sources. It has gained popularity among researchers and the industry and is one of the most used single-phase multilevel topologies [10,11]. Al-Haddad et al. presented the initial prototype of the PUC inverter in [12]. However, the seven-level-packed U-cell (PUC7) requires a complicated controller and many feedback sensors. A new sensorless five-level PUC inverter has been developed to address this issue. It has self-voltage capacitor balancing performance, a low-complexity modulation technique, and a simple control scheme, which makes it more attractive than the PUC7 [13,14]. Hence, various linear and nonlinear control techniques based on PI, model predictive control (MPC), and Lyapunov-based model predictive control have been implemented for grid-connected and standalone systems [15]. Despite their efficiency in controlling systems, PI and model-predictive MPC controllers can encounter issues related to uncertainties and disturbances. These issues can manifest as steady-state errors and voltage or current distortions, which can compromise the performance of the controlled system. Therefore, accounting for uncertainties and disturbances in designing and implementing PI and MPC controllers is important to ensure optimal system performance [16–18].

The paper presents a novel approach to control a single-phase grid-connected PUC5 using Lyapunov Control Theory (LCT) and a sensorless modulation strategy. The key aim of the control strategy is to maintain the PV panel operating at its maximum power output using an MPPT technique while also ensuring stable and high-quality injection of the grid current. To achieve this, the proposed method adjusts the capacitor voltage to half of the input voltage, resulting in good dynamic performance. The control strategy is based on the Lyapunov control theory, a powerful tool for designing control systems with guaranteed stability and performance. The sensorless modulation strategy eliminates the need for feedback sensors, simplifying the control system and reducing costs [19]. The study's results demonstrate the effectiveness of the proposed technique, which maintained the PV panel's output at its maximum power under both stable and variable conditions. Additionally, the method achieved high-quality injection of grid current, meeting the desired reference levels.

The article is organized as follows: section 2 presents a detailed description of the PUC5 inverter topology, including a theoretical analysis of its key features and operational principles. Section 3 focuses on modeling the PV

[1] LSPIE Laboratory, Faculty of Technology, University of Batna 2, Algeria.
[2] Higher National school of Renewable Energy, Environment and Sustainable Development, Constantine Road, Fesdis, Batna, 05078, Algeria.
[3] LAADI Laboratory, Faculty of Science and Technology, Djelfa University, Algeria.
[4] Laboratoire LTI, Université de Picardie Jules Verne, GEII, IUT de l'Aisne, 02880 Cuffies, France.
Emails: b.hadmar@univ-batna2.dz, s.drid@hns-re2sd.dz, kouzouabdellah@ieee.org, larbi.alaoui@u-picardie.fr

DOI: 10.59277/RRST-EE.2024.69.2.3

system. Section 4 discusses the modulation technique used. In section 5, a nonlinear controller is designed using Lyapunov theory. The simulation results are presented and discussed in section 6. Finally, section 7 presents the conclusion.

2. PUC5 CONFIGURATION

The PUC5 inverter configuration, as depicted in Fig. 1, consists of six power switches, one separate dc source (PV panel Vpv = 2E), and a capacitor as a second dc source (Vc = E).

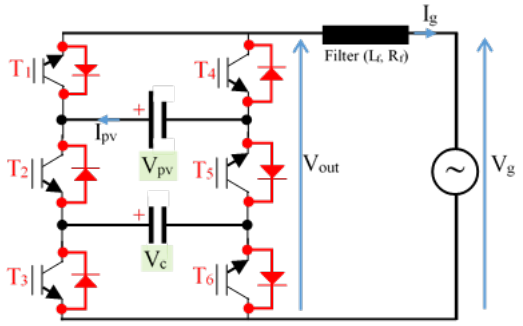

Fig. 1 – PUC5 configuration.

Table 1 depicts the switching state of the PUC5 inverter. Demonstrating that eight states (T1 & T4, T2 & T5, and T3 & T6) operate in complementary pairs. To obtain a balanced charging and discharging period for the capacitor and generate three voltage levels of (0, ±E, ±2E) with the technique proposed, the capacitor must be set to half the DC source (PV panel), which enables the output to generate five levels.

Table 1

The switching configurations and the output voltages of the PUC5

State	T1	T2	T3	Vout
1	1	0	0	2E
2	1	0	1	+E
3	1	1	0	+E
4	1	1	1	0
5	0	0	0	0
6	0	0	1	-E
7	0	1	0	-E
8	0	1	1	-2E

3. PV SYSTEM MODELING

The PUC topology under investigation has a specific configuration that requires each inverter leg to have a continuous and independent dc power source. To satisfy this requirement, the dc source for the upper voltage V1 represents the dc source generated by PV panels connected to a boost converter.

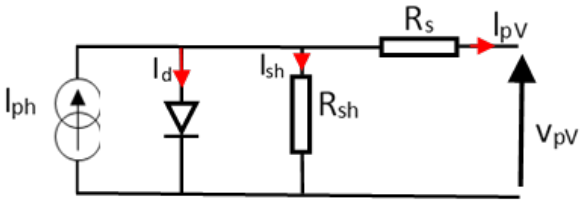

Fig. 2 – Electrical circuit of PV cell with one diode.

To enhance and optimize the control system's performance for the PV system, an MPPT method based on (P&O) algorithm was employed to reach the maximum power point of the PV system. It shows less complexity in comparison with other methods. The equivalent electrical circuit of the standard single-diode model is presented in Fig. 2 [1,3].

The following relation describes the mathematical model used to operate the PV-G.

$$\begin{cases} I_{pv} = I_{ph} - I_d - I_{sh} \\ I_d = I_s \left[exp\left(\frac{q\left(U_{pv}+(I_{pv}.R_s)\right)V_{pv}}{nKT} \right) - 1 \right] \\ I_{sh} = \frac{U_{pv}+(I_{pv}.R_s)}{R_{sh}} \end{cases} \quad (1)$$

The mathematical model for the photovoltaic generator (PV-G) involves several parameters, including V_{pv}, I_{pv}, I_{ph}, I_s, R_s, R_{sh}, q, K, and n. These parameters respectively represent the voltage (V) and output current (A) of the panel, the photocurrent (A), the reverse saturation current of the diode (A), the series resistance (Ω), the shunt resistance (Ω), the charge of an electron ($1.6 \cdot 10^{-19}$ C), the Boltzmann constant ($1.38 \cdot 10^{-23}$ J/K), and the quality factor of the diode. The electrical characteristics of the studied PV module BP SX 150 W, 8 series modules, and one parallel string are presented in Table 2 for reference.

Table 2

Electrical characteristics of the PV module BP SX 150:
8 modules in series; 1 string in parallel.

Parameter	Value
Maximum power Pmax	1200 W
Voltage at Pmax Vmp	34,5 V
Current at Pmax Imp	4,35 A
Short circuit current Isc	4,75 A
Open circuit voltage Voc	348 V
Temperature coefficient Isc	0,065 ± 0,015 %/°C
Temperature coefficient Voc	-160 ±20 mV%/°C
Temperature coefficient of power	-0,5 ±0,05 %/°c
NOCT	47 ±2 °C

Figures 3, 4, and 5 illustrate the current-voltage and power-voltage relationships for the PV module 5. These characteristic curves demonstrate the behavior of the PV-G under varying temperatures and irradiance.

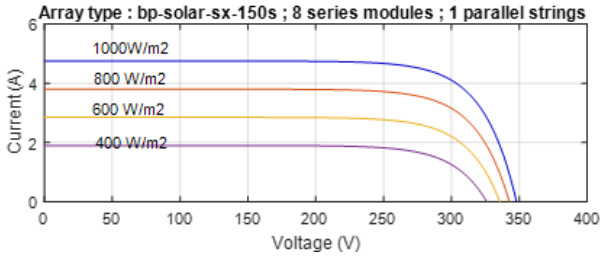

Fig. 3 – Effect of the irradiations on the I-V characteristic.

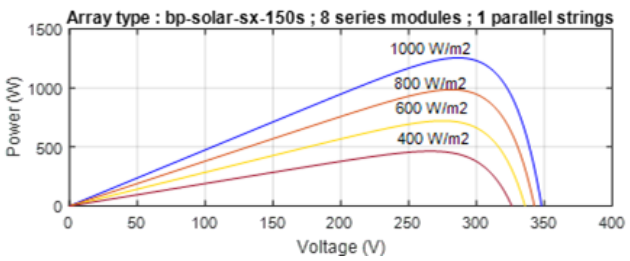

Fig. 4 – Effect of the irradiations on the P-V characteristic.

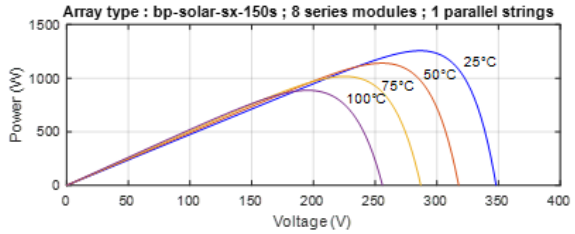

Fig. 5 – Effect of the temperature on the P-V characteristic.

4. SENSORLESS MODULATION APPROACH FOR PUC5 INVERTERS.

The suggested sensorless switching technique employs two level-shifted carriers and logic blocks, eliminating the need for a switching table. This technique can be implemented easily on low-cost microcontrollers without requiring complex computations. Furthermore, it ensures balanced charging and discharging of the capacitor throughout each switching cycle, reducing the size of the capacitor and improving power density. Consequently, the PUC inverter becomes smaller, cheaper, and capable of faster sensorless capacitor voltage balancing. Figure 6 presents the PUC switching interface according to the modulation approach proposed by [20].

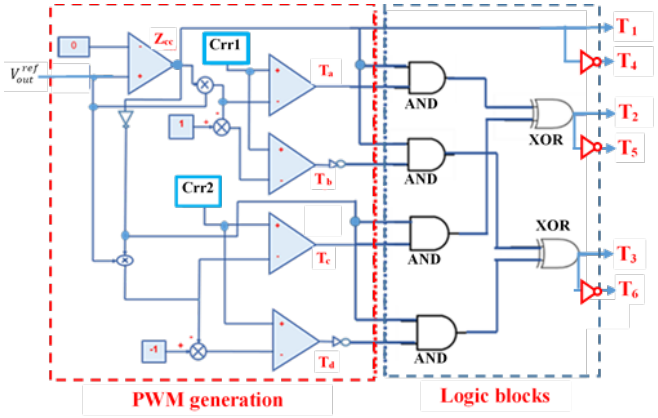

Fig. 6 – Scheme of the PUC switching interface modulation strategy.

Figure 7 presents the modulation strategy. A zero-crossing comparator reliably detects the positive half cycle of the reference voltage (Vrefout). This allows for controlling the semiconductor switches (T1,T4) at the fundamental frequency, resulting in efficient power conversion. The comparator output (Z_{cc}) is employed to determine the switching of eq.s (2) and (3).

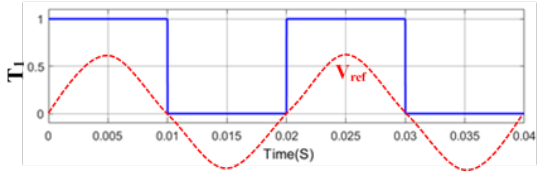

Fig. 7 –Block diagram of the modulation strategy technique.

$$Z_{cc} = \begin{cases} 0 & if\ V_{ref} \le 0 \\ 1 & if\ V_{ref} > 0 \end{cases} \quad (2)$$

$$T_1 = \bar{T}_4 = Z_{cc} \quad (3)$$

In Fig 8, the two triangular signals used for PWM comparisons are displayed. These signals are named Crr1 and Crr2, representing positive and negative triangular carrier signals that are level-shifted. It is significant to know that Crr1 and Crr2 are critical components of the proposed PWM strategy. The signals Ta, Tb, Tc, and Td can be expressed using equations, which are essential for analyzing and simulating the performance of the modulation strategy.

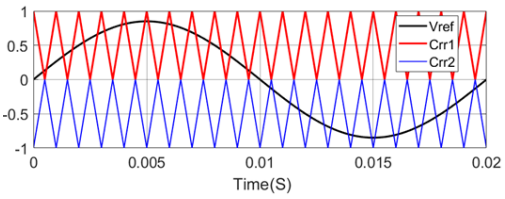

Fig. 8 – PWM carries with a reference voltage.

By utilizing these level-shifted carrier signals and the corresponding equations (4, 5, 6 and 7), the PWM strategy can effectively control the power switches, thereby achieving high efficiency and reduced harmonic distortion.

$$T_a = \begin{cases} 1 & \text{if } C_{rr1} \ge Z_{cc} . V_{ref} \\ 0 & \text{if } C_{rr1} < Z_{cc} . V_{ref} \end{cases} \quad (4)$$

$$T_b = \begin{cases} 1 & \text{if } C_{rr1} \ge \left(1 - Z_{cc} . V_{ref}\right) \\ 0 & \text{if } C_{rr1} < \left(1 - Z_{cc} . V_{ref}\right) \end{cases} \quad (5)$$

$$T_c = \begin{cases} 1 & \text{if } C_{rr2} \ge \bar{Z}_{cc} . V_{ref} \\ 0 & \text{if } C_{rr2} \ge \bar{Z}_{cc} . V_{ref} \end{cases} \quad (6)$$

$$T_d = \begin{cases} 1 & \text{if } C_{rr2} \ge \left(1 - \bar{Z}_{cc} . V_{ref}\right) \\ 0 & \text{if } C_{rr2} < \left(1 - \bar{Z}_{cc} . V_{ref}\right) \end{cases} \quad (7)$$

Equations (8) and (9) mathematically express the logic operations performed by the XOR (Exclusive OR) and AND gates, respectively.

$$T_2 = \bar{T}_5 = (T_a . Z_{cc}) \oplus (T_a . \bar{Z}_{cc}) \quad (8)$$

$$T_3 = \bar{T}_6 = (\bar{T}_b . Z_{cc}) \oplus (\bar{T}_b . \bar{Z}_{cc}) \quad (9)$$

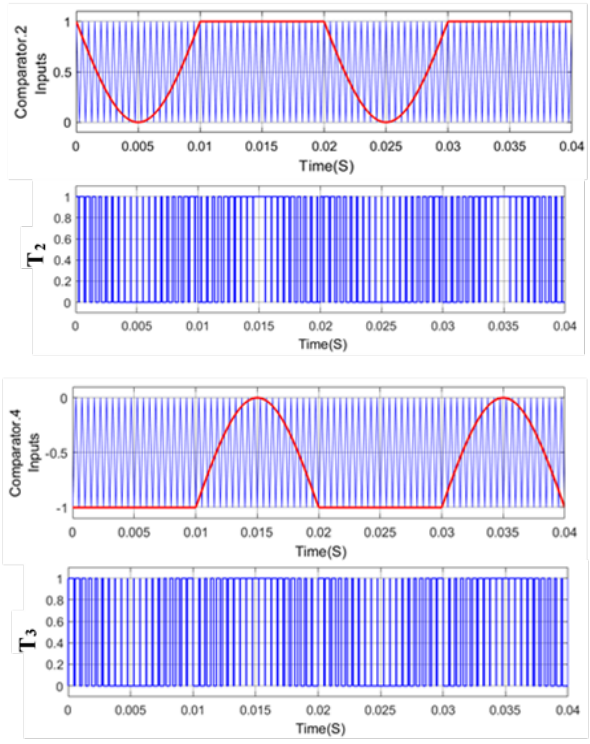

Fig. 9 – Modulation strategy.

The XOR gate takes two input signals and generates an output signal that is high ("1") when the two inputs are different and low ("0") when the two inputs are the same. The AND gate, on the other hand, takes two input signals and generates an output signal that is high ("1") only when both inputs are high ("1") and low ("0"). Otherwise, the results are presented in Fig. 9.

5. LYAPUNOV CONTROLLER-BASED ON SENSORLESS MODULATION TECHNIQUE FOR GRID-CONNECTED PUC5 INVERTER

The mathematical nonlinear model represented by (10) can be derived using Kirchhoff's voltage law applied between point A and point B, displayed in Fig. 1, following the principle of the grid-connected PUC5 topology:

$$\begin{cases} \dfrac{dI_g}{dt} = \dfrac{1}{L_f}\left(V_{out} - R_f\, I_g - V_g\right), \end{cases} \tag{10}$$

where V_g is the grid voltage, while V_{out} represents the PUC-5 output voltage. The grid filter's resistance and inductance are denoted by (R_f, L_f). The Lyapunov function provided in (11) must be positive definite to design the control law.

$$V(e) = \frac{1}{2}\, e_i^2 > 0\,, \quad \forall e_i\,, \tag{11}$$

where (e_i) is the grid current error (12) defined as:

$$\begin{cases} e_i = (I_g - I_g^{ref}), \\ \dot{e}_i = (\dot{I}_g - \dot{I}_g^{ref}). \end{cases} \tag{12}$$

Equation (13) presents the Lyapunov function derivate, computed using the difference between the grid current and its intended reference signal.

$$\dot{V}(e_i) = e_i \dot{e}_i = e_i(\dot{I}_g - \dot{I}_g^{ref}). \tag{13}$$

If we replace (10) in (13)

$$\dot{V}(e_i) = e_i\left(\frac{1}{L_f}\left(V_{out} - R_f\, I_g - V_g\right) - \dot{I}_g^{ref}\right). \tag{14}$$

The derivative Lyapunov function should be negative to guarantee the overall system's stability. To ensure this condition, the second part of (14) should be

$$\left(\frac{1}{L_f}\left(V_{out} - R_f\, I_g - V_g\right) - \dot{I}_g^{ref}\right) = Ke_i, \tag{15}$$

where $K > 0$.

Then the derivative Lyapunov function becomes (16)

$$\dot{V}(e_i) = -K\, e_i^2 < 0\,, \quad \forall e_i\,. \tag{16}$$

The control law shown in (17) is obtained from (15). The proposed robust control law in (17) provides global asymptotic stability for the PUC5 control loop.

$$V_{out} = L_f(Ke_i + \frac{1}{L_f} R_f\, I_g + \frac{1}{L_f} V_g + \dot{I}_g^{ref}). \tag{17}$$

The global scheme of the overall control system is illustrated in Fig. 10. In this figure, the reference current of grid (I_g^{ref}), which is obtained for the MPPT controller and modulated with grid frequency using a phase-locked loop (PLL). The grid voltage angle is measured by PLL to synchronize the inverter current with grid frequency and voltage. Then (I_g^{ref}) is used in the grid current loop via the proposed controller in equation (17). After that V_{out} is used as input of the switching interface modulation strategy (see Fig. 6) to control the PUC-5.

In Fig. 10, the inverter current and grid voltage are measured for application to the robust controller.

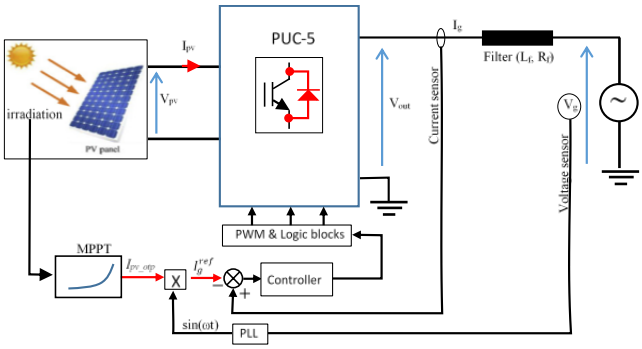

Fig. 10 – Global scheme of the overall control system.

The voltage sensorless switching technique keeps the capacitor voltage at half the PV panel voltage.

6. SIMULATION RESULTS

To assess the effectiveness and efficiency of the proposed Lyapunov controller, which utilizes a sensorless switching technique, we conducted simulations on a 5-level grid-connected PUC inverter using the PowerSystems toolbox of MATLAB software, as shown in Fi. 11. The system parameters required for the testing are listed in Table 3 for reference.

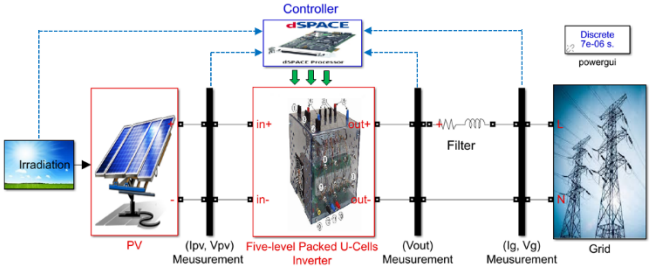

Fig. 11 – Block diagram of the PUC5 of the implemented proposed controller.

Table3

The simulation parameters

Grid Voltage Vg	220 V
DC Capacitor v2	1000 µF
Switching frequency	3000 Hz
Grid frequency	50 Hz
Grid Side Resistor Rg	0.2 mΩ
Grid Side Indictor Lg	2 mH

In this study, the performance of a photovoltaic (PV) system was assessed by subjecting a PV string to a step change in solar irradiance from 1000 W/m² to 800 W/m², while also reducing it to 600 W/m² as shown in Fig. 12. The PV output voltage, current, and power were displayed in Fig. 13, 14 and 15 as the solar irradiance varied. Analysis of Fig. 16 indicates that the capacitor voltages remained constant at half of the upper voltage source Vpv, and the steady-state error margin was significantly reduced to below 5%. This improvement was achieved through the proposed

Lyapunov controller based on the sensorless switching method.

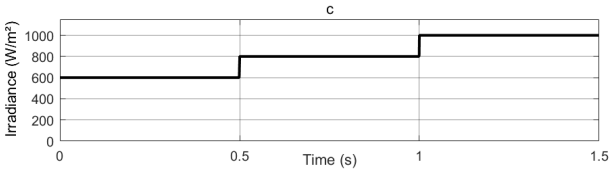

Fig. 12 – Irradiance step change test.

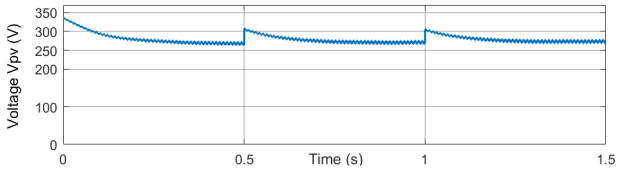

Fig. 13 – Voltage response of PV under irradiation variation.

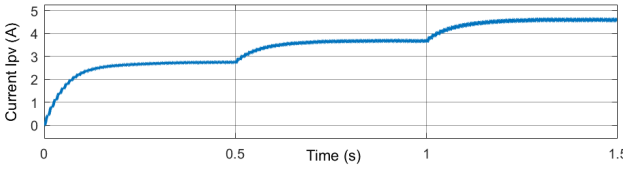

Fig. 14 – PV Current under irradiation variation.

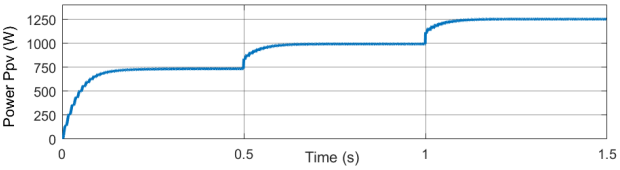

Fig. 15 –Power of PV under irradiation variation.

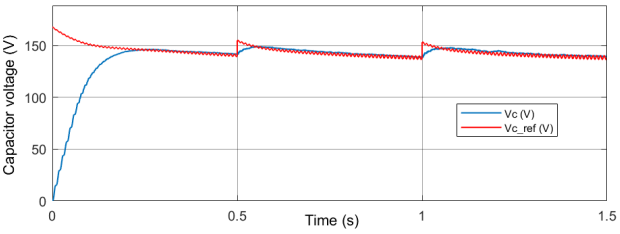

Fig. 16 – The transient of the capacitor voltage V_C.

Figure 16 shows the transient state of the capacitor voltage V2, which self-balances quickly after a disturbance. This further demonstrates the effectiveness and robustness of our proposed technique. These figures comprehensively overview the PUC5 inverter's performance under various operating conditions.

In Fig. 17 and 18, we observe that the injected current has high tracking quality against its reference, indicating the effectiveness of our proposed control strategy. Moreover, the same figures present the output voltage of the PUC5 inverter, demonstrating the effectiveness of our proposed control technique in maintaining stable and high-quality output voltage.

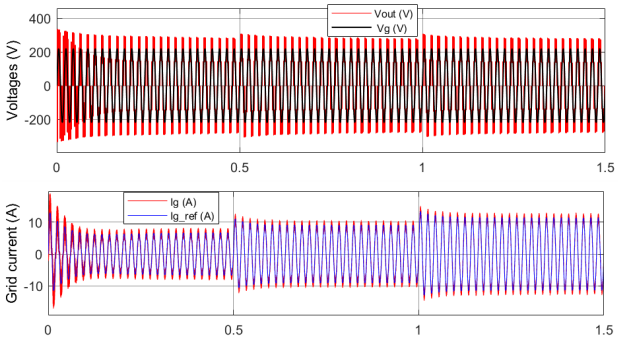

Fig. 17 – PUC5 voltage and current generating with the grid voltage.

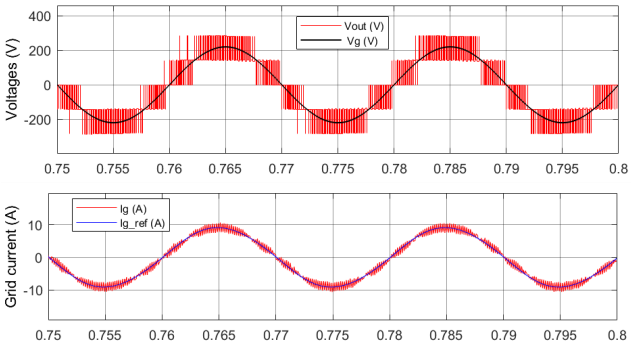

Fig. 18 – Zoom PUC5 voltage and current generating with the grid voltage.

Figure 19 shows that the grid current's harmonic content (THD) is around 2.7 %, within the acceptable range for power quality. In addition, Fig. 20 shows the reduced THD (0.55 %) of the PUC5 converter output voltage, highlighting the system's ability to minimize harmonic distortion.

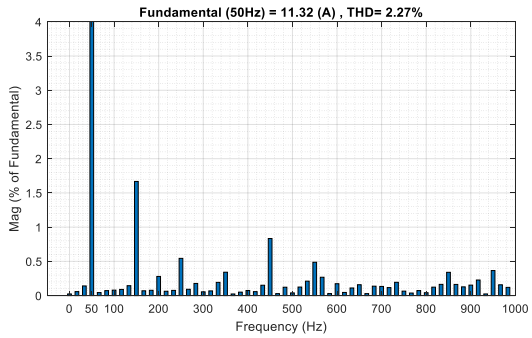

Fig. 19 –FFT analysis of the grid current (ig).

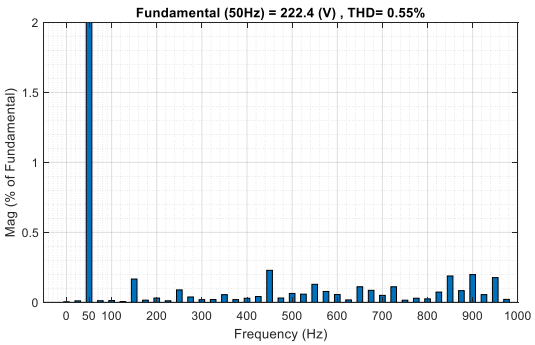

Fig. 20 –FFT analysis of the output voltage.

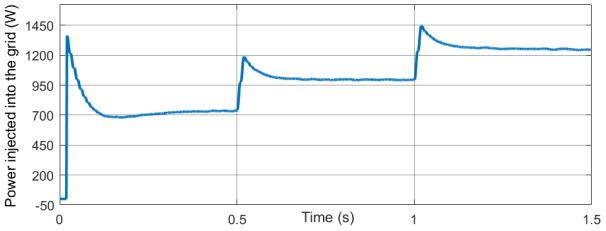

Fig. 21 – Output voltage, grid current and power injected to the grid at ac side transient test under an irradiance step change.

Figure 21 shows the transient operation when the irradiance shifts from 600 W/m² to 800 W/m² and then to 1000 W/m². The variables in this figure exhibit rapid transient responses, indicating the system's high responsiveness to input disturbances. Moreover, Fig. 17 illustrates that the output voltage and injected current are accurately synchronized with the grid voltage. The figures demonstrate the efficacy of our proposed control strategy in delivering consistent and high-quality grid current injection.

7. CONCLUSIONS

This study presented a sensorless modulation technique for grid-connected PUC5 inverters based on the Lyapunov control technique. The suggested control technique achieved the asymptotic stability of the system and efficient grid current tracking while maintaining the capacitor voltage at its desired values in a transient and steady state. Moreover, it allows for reduced harmonic distortion. The robustness analysis demonstrated resilience against step changes of irradiation, with minimal impact on the system performance. Simulation results validated the effectiveness of the proposed technique. In the future, this work will be implemented in a real-time system.

Received on 18 July 2023

REFERENCES

1. L. Chrifi-Alaoui, S. Drid, M. Ouriagli, D. Mehdi, *Overview of photovoltaic and wind electrical power hybrid systems*, Energies, **16**, *12* (2023).
2. F. Mechnane, S. Drid, N. Nait-Said, L. Chrifi-Alaoui, *Robust current control of a small-scale wind-photovoltaic hybrid system based on the multiport dc converter*, Applied Sciences, **13**, *12* (2023).
3. M. Ilie, D. Floricau, *Grid-connected photovoltaic systems with multilevel converters-molding and analysis*, Rev. Roum. Sci. Techn. – Électrotechn. Et Énerg., **68**, 1, pp. 77–83 (2023).
4. D. Beriber, A. Talha, A. Kouzes, *Multilevel inverter for grid-connected photovoltaic*, Rev. Roum. Sci. Techn. – Électrotechn. Et Énerg., **62**, *2*, pp. 105–110 (2022).
5. D. Ragul, V. Thiyagarajan, *A novel fault-tolerant asymmetrical 21-level inverter topology reduced componts*, Rev. Roum. Sci. Techn. – Électrotechn. Et Énerg., **68**, 2, pp. 200–205 (2023).
6. B. Aljafari, K. Rameshkumar, V. Indragandhi, *A novel single-phase shunt active power filter with a cost function-based model predictive current control technique*, Energies, **15**, pp. 4531, (2022).
7. A. Azeem, M. Tariq, K. A. Lodi, C. Bharatiraja, *Performance analysis of discontinuous pulse width modulation schemes on PUC-5 inverter*, Second IEEE Conference on Power Electronics, Intelligent Control and Energy Systems (SPICES), Delhi, India, pp. 636–641 (2018).
8. H. Vahedi, M. Sharifzadeh, K. Al-Haddad, *Modified seven-level pack U-cell inverter for photovoltaic applications*, IEEE Journal of Emerging and Selected Topics in Power Electronics, **6**, *3*, pp. 1508–1516 (2018).
9. M. Seyedmahmoudian, S. Mekhilef, R. Rahmani, R. Yusof, E.T. Renani, *Analytical modeling of partially shaded photovoltaic systems*, Energies, **6**, *3*, pp.128–144 (2013).
10. M. Sharifzadeh, H. Vahedi, K. Al-Haddad, *New constraint in SHE-PWM for single-phase inverter applications*, IEEE Transactions on Industry Applications, **54**, *3*, pp. 4554-4562, (2018).
11. B. Hadmer, S. Drid, A. Kouzou, F. Mechnane, L. Chrifi-Alaoui, M.D. Drid, *SPWM and third harmonic injection techniques for 7-level packed U-cell inverter,* IEEE, 21st International Conference on Sciences and Techniques of Automatic Control and Computer Engineering (STA), Sousse, Tunisia, pp. 508–511 (2022).
12. Y. Ounejjar, K. Al-Haddad, L.A. Gregoire, *Packed U-cells multilevel converter topology: theoretical study and experimental validation*, IEEE Transactions on Industrial Electronics, **58**, *4*, pp. 1294–1306 (2010).
13. B. Hadmer, S. Drid, A. Kouzou, F. Mechnane, L. Chrifi–Alaoui, M.D. Drid, *Voltage sensorless sliding mode control for five level PUC single phase inverter used in PV system*, IEEE, 21st International Conference on Sciences and Techniques of Automatic Control and Computer Engineering (STA), Sousse, Tunisia, pp. 492–497(2022).
14. M. Abarzadeh, H. Vahedi, K. Al-Haddad, *Fast sensor-less voltage balancing and capacitor size reduction in PUC5 converter using novel modulation method*, IEEE Transactions on Industrial Informatics, **15**, *8*, pp. 4394–4406 (2019).
15. M. Babaie, M. Sharifzadeh, M. Mehrasa, K. Al-Haddad, *Optimized based algorithm first order sliding mode control for grid-connected packed e-cell (PEC) inverter*, 2019 IEEE Energy Conversion Congress and Exposition (ECCE), pp. 2269–2273 (2019).
16. A. Chebabhi, A.A.M. Al-Dwa, M. Defdaf, *New modeling and enhanced control strategy for grid-connected four-leg inverter without phase-locked loop and park's transformation*, Rev. Roum. Sci. Techn. – Électrotechn. Et Énerg., **68**, 2, pp. 121–126 (2023).
17. A. Krama, S.S. Refaat, H. Abu-Rub, *A robust second order sliding mode control of sensorless five-level packed U-cell inverter*, IEEE, the 46th Annual Conference of the IEEE Industrial Electronics Society (IECON), Singapore, pp. 2412–2417 (2020).
18. D. Sakri, H. Laib, S.E. Farhi, N. Golea, *Sliding mode approach for control and observation of a three-phase AC-DC pulse-width modulation rectifier*, Electrical Engineering & Electromechanics, **2**, pp. 49–56 (2023).
19. M. Babaie, M. Sharifzadeh, M. Mehrasa, G. Chouinard, K. Al-Haddad, *Adaptive neural fuzzy inference system controller for seven-level packed U-Cell inverter*, 45th Annual Conference of the IEEE Industrial Electronics Society (IECON), Lisbon, Portugal, **1**, pp. 3505–3510.
20. M. Abarzadeh, S. Peyghami, K. Al-Haddad, N. Weise, L. Chang, F. Blaajberg, *Reliability and performance improvement of PUC converter using a new single-carrier sensor-less PWM method with pseudo reference functions*, IEEE Transactions on Power Electronics, **36**, *5*, pp. 6092–6105 (2020).
21. M. Babaie, M. Sharifzadeh, M. Mehrasa, K. Al-Haddad, *Lyapunov-based neural network estimator designed for grid-tied nine-level packed E-cell inverter*, IEEE, Applied Power Electronics Conference and Exposition (APEC), New Orleans, LA, USA, pp. 3311–3315 (2020).
22. H. Makhamreh, M. Sleiman, O. Kükrer, K. Al-Haddad, *Lyapunov-based model predictive control of a PUC7 grid-connected multilevel inverter*, IEEE Transactions on Industrial Electronics, **66**, *9*, pp. 7012–7021 (2018).